Histol Histopathol (2023) 38: 1403-1413

Histology and Histopathology
From Cell Biology to Tissue Engineering

ORIGINAL ARTICLE Open Access

MiR-5195-3p functions as a tumor suppressor by targeting RHBDD1 in ovarian cancer

Zhanyu Wang, Xiaoping Zhang, Yongying Liu, Xiaoyan Shi, Lijun Li, Yun Jia, Fangfang Wu, Haosen Cui and Liang Li

Department of Gynecology and Obstetrics, Fuyang Hospital of Anhui Medical University, Fuyang, Anhui Province, China

Summary. Background. Recent studies have reported the tumor suppressive role of miR-5195-3p in the progression of several cancers, but the potential roles of miR-5195-3p in ovarian cancer (OC) remain largely unknown.

Methods. We first analyzed the expression levels of miR-5195-3p in 83 pairs of human OC tissues and adjacent specimens by reverse transcription-quantitative PCR. The correlation of miR-5195-3p/rhomboid domain containing 1 (RHBDD1) and clinicopathological parameters was analyzed by chi-square test. The prognostic value of miR-5195-3p was evaluated by Kaplan-Meier method Cox proportional hazards models. The effects of miR-5195-3p on cell proliferation, cell cycle distribution, migration and invasion were examined by CCK-8 assay, colony formation assay, flow cytometry and transwell assay. Tumor forming was evaluated by nude mice model *in vivo*. The association between miR-5195-3p and RHBDD1 was verified by luciferase reporter assay.

Results. We observed that miR-5195-3p level was remarkably reduced in OC tissues as compared to adjacent tissues. The expression of miR-5195-3p was associated with FIGO stage, depth of invasion and poor survival prognosis in OC patients. Overexpression of miR-5195-3p significantly suppressed cell proliferation, cell cycle G1/S transition, migration and invasion in OC cell lines (SKOV-3 and OVCAR3), while knockdown of miR-5195-3p obtained the opposite results. We further confirmed miR-5195-3p as a negative post-transcriptional modulator of RHBDD1. RHBDD1 expression was upregulated in OC tissues compared with adjacent tissues, which was inversely correlated with miR-5195-3p expression. The expression of RHBDD1 was associated with FIGO stage and distant metastasis. RHBDD1 overexpression reversed the suppressive role of miR-5195-3p on OC cell proliferation, migration and invasion. Consistent with the *in vitro* results, miR-5195-3p overexpression decreased the growth of subcutaneously inoculated tumors in nude mice.

Conclusions. Taken together, the present results indicated that miR-5195-3p acts a tumor suppressor by targeting RHBDD1 in OC.

Key words: Ovarian cancer, miR-5195-3p, RHBDD1, Prognosis, Cell functions

Corresponding Author: Liang Li, Department of Gynecology and Obstetrics, Fuyang Hospital of Anhui Medical University, No.99 Huangshan Road, Hefei Modern Industrial Park, Yingzhou District, Fuyang 236000, Anhui Province, China. e-mail: li_liang3443@outlook.com

www.hh.um.es. DOI: 10.14670/HH-18-595

Introduction

Ovarian cancer (OC) ranks first in the mortality of gynecological malignancies that pose a major threat to women's livers (Siegel et al., 2020). It has been reported that approximately 20% of OC patients are diagnosed at early stage for its insidious symptoms but most of patients are detected for the first time at the advanced stage (Boussios et al., 2020). Although the therapeutic efficacy of OC patients has been improved under the treatment standard of surgery combined with platinum-based chemotherapy (Armstrong et al., 2021), the five-year survival of advanced OC still remain 10-20% with high recurrence rate (Koole et al., 2019; Xie et al., 2020; Yousefi et al., 2020). Therefore, it is urgent to investigate the potential molecular mechanisms underlying the malignant progression of OC.

MicroRNA (miRNAs/miRs) represent a class of endogenous small non-coding RNAs with 21-25 nucleotides that participate in the post-transcriptional modification process via binding to their target messenger RNA (Griffiths-Jones et al., 2006). Extensive studies have indicated that miRNAs are frequently dysregulated in various types of cancer by acting as oncogenic genes or tumor suppressors (Bracken et al., 2016; Rupaimoole and Slack, 2017). In recent years, miR-5195-3p, a quite newly discovered miRNA, has been found to be abnormally expressed and participate in the regulation of the progression of multiple diseases. For instance, Yang (2019) reported that overexpression of miR-5195-3p repressed cell proliferation, migration

and invasion by directly targeting MYO6 in non-small cell lung cancer (NSCLC) cells. Jiang et al. (2017) revealed that miR-5195-3p suppressed the proliferation and invasion of human bladder cancer cells via suppression of KLF5. In addition, miR-5195-3p has been reported to be a tumor suppressor by targeting NEDD9 in osteosarcoma (Wang et al., 2019) and targeting BRIC2 in glioma cells (Yang et al., 2020). Interestingly, a recent report by Ebrahimi and Reiisi (2019) showed a significant reduction in miR-5195-3p expression in OC samples. However, the clinical significance and biological functions of miR-5195-3p in OC progression have not been fully elucidated until now.

The rhomboid protein family mainly consists of active proteases and inactive members lacking catalytic residues, which have been demonstrated to participate in physiological functions, including mitochondrial dynamics, growth factor signaling, inflammation and parasite invasion (Freeman, 2008, 2014). Rhomboid domain containing 1 (RHBDD1), a mammalian member of the rhomboid protein family, is highly responsible for regulating intramembrane proteolysis (Wang et al., 2008), which was recently reported to be associated with carcinogenesis. In brief, highly expressed RHBDD1 was not only correlated with poor prognosis, but also associated with uncontrolled tumor cell growth and metastasis in colorectal cancer (Han et al., 2015; Song et al., 2015; Zhang et al., 2018a). Similarly, RNA interference mediated RHBDD1 silencing inhibited cell proliferation and induced cell cycle arrest in human glioblastoma (Wei et al., 2014) and hepatocellular carcinoma (Liu et al., 2013) cells. Additionally, knockdown of RHBDD1 inhibited cell proliferation, G1/S phase transition, migration and invasion in breast cancer (Huang et al., 2018; Zhang et al., 2018b). RHBDD1 silencing inhibited cell growth and invasion of NSCLC by mediating the ZEB1/PI3K/AKT signaling pathway (Xu et al., 2021). Combined with the online prediction that RHBDD1 is a potential target of miR-5195-3p, we thus speculated that the miR-5195-3p/RHBDD1 axis might play an important role in the progression of OC.

Based on this hypothesis, we first determined the expression level of miR-5195-3p in OC tissues and analyzed the clinical significance of miR-5195-3p in OC patients. By performing a series of functional experiments, we further evaluated whether miR-5195-3p regulated OC cell proliferation, cell cycle progression, migration, invasion and tumor growth by targeting RHBDD1.

Materials and methods

Clinical samples

Eighty-three epithelial OC tissues and adjacent normal tissues, containing ovary (n=28), peritoneum (n=20) and ovarian surface epithelium (n=35) were harvested from OC patients at the Fuyang Hospital of Anhui Medical University (Anhui, China) between March 2016 and May 2019. Written informed consent was signed by each participant. These collected specimens were immediately frozen within liquid nitrogen. The clinicopathological information of 83 patients, including age, tumor size, FIGO stage and histopathological subtypes was recorded. The recruited patients had not yet received preoperative chemotherapy and/or radiation therapy. Patients were followed up for five years and the clinical assessment was performed in each patient. The present study was approved by the Ethics Committee of Fuyang Hospital of Anhui Medical University (Anhui, China).

Cell culture and transfection

Two OC cell lines (SKOV-3 and OVCAR3) were obtained from the American Type Culture Collection (ATCC, Manassas, VA, USA) and cultured in Roswell Park Memorial Institute 1640 (RPMI-1640, Gibco, Carlsbad, CA, USA) containing 10% FBS at 37°C in a humidified atmosphere containing 5% CO_2. The miR-5195-3p mimics, mimics negative control (NC), miR-5195-3p inhibitor and inhibitor NC were synthesized from Ribo Biotechnology Co. Ltd. (Guangzhou, China). RHBDD1 overexpressed plasmid (pcDNA3.1-RHBDD1) and empty vector pcDNA3.1 were purchased from GenePharma Co. Ltd (Shanghai, China). For transfection experiments, SKOV-3 and OVCAR3 cells were plated in a six-well plate with 5×10^5 cells per well. Cell transfection was performed for 48h with Lipofectamine 2000 reagent in accordance with the manufacturer's instructions (Thermo Fisher Scientific, Waltham, MA, USA).

Reverse transcription-quantitative PCR

Total tissues and cellular RNA was extracted using TRIzol reagent (Invitrogen, Carlsbad, CA, USA) and complementary DNA synthesis was performed with the PrimeScript RT reagent kit (TakaRa, Dalian, China) according to the manufacturer's protocol. Reverse transcription-quantitative PCR was conducted using miScript SYBR Green PCR kits (Qiagen, New York, NY, USA) for miRNA and SYBR Premix Ex Taq II (Takara Biotechnology, Dalian, China) for RHBDD1 mRNA with the following cycling parameters: initial denaturation for 3 min at 95°C, followed by 45 cycles of 5 s at 95°C and 30 s at 60°C. The primers for reverse transcription-quantitative PCR were miR-5195-3p, forward: 5′-TAGCAGACTCTTATGATG-3′ and reverse: 5′-TGGTGGAGTCGTCGTG-3′; U6, forward 5′-TAGGATTATACATTGTAAGAGGT-3′, reverse 5′-GTGTGCTACAGAATTTAAAGGTT-3′; RHBDD1, forward 5′-ACGCAGGCGGGTCGTA-3′, reverse 5′-GGGCCAAAGTTGCTAGGGT-3′; and GAPDH, forward 5′-GAACGGGAAGCTCACTGG-3′, reverse 5′-GCCTGCTTCACCACCTTCT-3′. The relative expression level of miR-5195-3p and RHBDD1 was

calculated and compared with the $2^{-\Delta\Delta Ct}$ method (A & B, 2001) after normalization with U6 and GAPDH, respectively.

Cell counting kit-8 (CCK-8) assay

Cell viability was assessed by CCK-8 assay in accordance with the manufacturer's instructions (Sigma-Aldrich, St. Louis, MO, USA). In brief, transfected cells at a density of 3,000 cells per well were inoculated into 96-well plates. A 10 μL CCK-8 solution was added 24, 48 and 72h later, respectively. After being cultured further for 2h at 37°C, the absorbance at 450 nm was measured using a microplate reader (BioTek Synergy, Winooski, VT, USA).

Colony formation assay

Transfected cells were seeded into six-well plates at a density of 500 cells per well and cultured for two weeks ensuring the replacement of the culture medium at 3-day intervals. Then, cells were fixed with 4% paraformaldehyde and stained with 0.1% (v/v) crystal violet for 15 min. Colonies containing ≥50 cells were counted through a microscope.

Cell cycle analysis

After 48h transfection, cells were rinsed by PBS and harvested after 5 min of centrifugation at 2000 rpm. Subsequently, 1 ml single-cell suspension containing 1×10^6 cells was prepared and the supernatant was further obtained after centrifugation. Next, the supernatant was fixed with 70% cold methanol overnight at 4 °C. After washing with PBS, cells were stained with 500 μL of PI/RNaseA staining solution (BD Biosciences, Bedford, MA, USA) and analyzed for cell cycle distribution by flow cytometry (BD Biosciences).

Transwell assays

The migratory and invasive abilities of transfected cells were evaluated using transwell chambers (8-μm; Millipore, Billerica, MA, USA), which were coated with (invasion assay) or without (migration assay) Matrigel (BD Biosciences) according to the manufacturer's protocol. In brief, 5×10^4 transfected cells re-suspended in serum-free medium were placed in the upper compartment, whereas the normal medium containing 20% FBS as the chemoattractant was added in the lower compartment. After incubation for 24 h, the cells located on the lower surfaces were fixed with methanol for 10 min and stained with 0.5% crystal violet. Then, the number of migratory/invasive cells was counted under an inverted microscope in five randomly selected fields.

Dual-luciferase reporter assay

Dual-luciferase reporter assay was performed to investigate whether miR-5195-3p could interact with the 3′-UTR of RHBDD1. Briefly, wild type (WT) 3′-UTR of RHBDD1 predicted to interact with miR-5195-3p or the mutant (MUT) RHBDD1 3′-UTR was amplified and inserted into pmirGlo vector (Promega, Madison, WI, USA) to construct WT RHBDD1 or MUT RHBDD1 constructs, respectively. Afterwards, the miR-5195-3p mimics or mimics NC and the pmirGlo constructs were co-transfected into SKOV-3 and OVCAR3 cells using the Lipofectamine 2000 transfection reagent (Invitrogen). After 48h co-transfection, cells were lysed and relative luciferase activities were calculated with the Dual-Luciferase Reporter Assay kit (Promega) according to the manufacturer's instructions.

Western blot analysis

Total protein sample was isolated from cells with RIPA lysis buffer (Thermo Fisher Scientific, MA, USA) and protein concentrations were quantified by a BCA Protein Assay kit (Thermo Fisher Scientific). Approximately 30 μg of proteins were separated by 10% SDS-PAGE and then electroblotted onto PVDF membranes (Millipore). The membranes were blocked with 5% non-fat milk and incubated with primary antibodies against RHBDD1 (1:5,000; Sigma-Aldrich, St. Louis, MO, USA) and GAPDH (1:50,000; Proteintech, Chicago, IL, USA) overnight at 4°C, followed by incubation with horseradish peroxidase (HRP)-conjugated goat anti-rabbit secondary antibody (1:5000, SC-2054, Santa Cruz, CA, US) at room temperature for 2h. After washing with PBS twice, the protein bands were visualized with an enhanced chemiluminescence substrate (Millipore).

Animal experiments

Five-week-old male BALB/c nude mice were purchased from the Animal Husbandry Center of the Shanghai Institute of Cell Biology (Shanghai, China). For xenograft tumor model, SKOV-3 and OVCAR3 cells transfected with miR-5195-3p mimics or mimics NC were cultured in fresh RPMI-1640 medium under normal conditions. After being anesthetized with 1% isoflurane, mice were subcutaneously inoculated with 5×10^6 transfected SKOV-3 and OVCAR3 cells diluted in 0.2 ml PBS into the right flank of each nude mouse. Subcutaneous tumor growth was measured every 7 days with a caliper for 35 days using the formula: volume=1/2 (length × width^2). Subsequently, euthanasia was carried out by cervical dislocation after rendering nude mice unconscious with CO_2, and tumors were dissected and weighed. The expression levels of miR-5195-3p and RHBDD1 were detected between miR-5195-3p mimics and mimics NC group by reverse transcription-quantitative PCR analysis. All experimental procedures were performed according to the regulations and internal biosafety and bioethics guidelines of Fuyang Hospital of Anhui Medical University.

Statistical analysis

All data were analyzed using GraphPad Prism 6.0 and expressed as mean ± standard deviation. The association between clinicopathological parameters and miR-5195-3p expression was analyzed using chi-square test as appropriate. Kaplan-Meier method was used to evaluate the survival rate and analyzed by log-rank test. Survival data were evaluated using univariate and multivariate Cox proportional hazards models. Pearson's correlation analysis was performed to analyze the correlation between miR-5195-3p and RHBDD1 in OC tissues. The significant differences between two groups were analyzed by Student's t-test, and between multiple groups were analyzed by one-way analysis of variance followed by the Tukey test. $P<0.05$ was considered to indicate a statistically significant difference.

Results

MiR-5195-3p expression was notably reduced and associated with poor prognosis of OC patients

The expression levels of miR-5195-3p were determined by reverse transcription-quantitative PCR in 83 pairs of matched OC tissues and adjacent tissues, independently. As shown in Figure 1A, miR-5195-3p level was remarkably reduced in OC tissues as compared to adjacent tissues. We further divided patients into high expression group (n=41) and the low expression group (n=42), based on the median value of miR-5195-3p. The relationship of miR-5195-3p with the clinicopathological characteristics of OC was analyzed and is summarized in Table 1. It could be informed that the expression of miR-5195-3p was related to FIGO stage (P=0.043) and depth of invasion (P=0.044). We further explored the correlation of miR-5195-3p expression with overall survival of OC patients by performing Kaplan-Meier analyses. The results showed that patients expressing a low level of miR-5195-3p presented worse prognosis as opposed to those who showed high expression of miR-5195-3p (P=0.0162, Fig. 1B). Univariate and multivariate analysis demonstrated that FIGO stage, depth of invasion and miR-5195-3p were independent risk factors for overall survival in OC patients (Table 2).

MiR-5195-3p inhibits cells proliferation, migration and invasion in OC cells

To investigate the effects of miR-5195-3p on the biological behavior of OC cells, we overexpressed and silenced miR-5195-3p by transfecting miR-5195-3p mimics and inhibitor, respectively in SKOV-3 and OVCAR3 cell lines. First, reverse transcription-quantitative PCR was utilized to confirm the transfection

Table 1. Correlations between miR-5195-3p expression and clinicopathological characteristics in OC patients.

Patient characteristics	Cases (n=83)	Expression of miR-5195-3p		P value
		Low (n=42)	High (n=41)	
Age				0.991
<55	35	21	14	
≥55	48	21	27	
Tumor size (cm)				0.952
<5	51	30	21	
≥5	32	12	20	
FIGO stage				0.043*
Early (I-IIA)	37	9	28	
Advanced (IIB-IV)	46	33	13	
Tumor differentiation				0.100
Good/moderate	53	25	28	
Poor/undifferentiated	30	17	13	
Histopathological subtypes				0.119
Serous	70	38	32	
Mucinous and othersa	13	4	9	
Depth of invasion				0.044*
T1-T2	43	12	31	
T3-T4	40	30	10	
Distant metastasis				0.123
Negative	45	14	31	
Positive	38	28	10	
Histological grade				0.994
Low/moderate	59	27	32	
High	24	15	9	

*$P<0.05$ (p values are calculated with chi-square test); OC, ovarian cancer; FIGO Federation International of Gynecology and Obstetrics. aothers: others include the endometrioid, clear cell, and undifferentiated ovarian cancers.

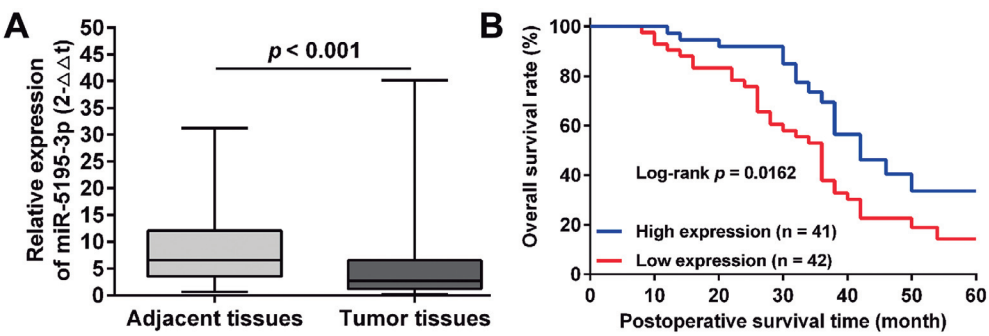

Fig. 1. MiR-5195-3-5p downregulation in ovarian cancer indicates poor prognosis. **A.** Relative expression of miR-5195-3p of ovarian cancer samples and adjacent normal tissues (n=83), assessed by reverse transcription-quantitative polymerase chain reaction. **B.** Kaplan-Meier survival curves of OC cases with overexpressed (n=41) and reduced (n=42) miR-5195-3p expression. P=0.0162 assessed using log-rank test.

Table 2. Univariate and multivariate analysis of factors associated with overall survival in patients with OC.

Characteristics	Univariate analysis		Multivariate analysis	
	HR (95% CI)	P value	HR (95% CI)	*P* value
Age (≥55 vs. <55 year)	1.123 (0.925-1.642)	0.562	NA	NA
Tumor size (≥5 vs. <5 cm)	1.265 (0.986-2.015)	0.165	NA	NA
FIGO stage (I/IIA vs. <IIB/IV)	0.135 (0.098-0.265)	0.003*	0.362 (0.105-0.621)	0.015*
Tumor differentiation (Good/moderate vs. Poor/undifferentiated)	1.025 (0.798-1.452)	0.265	NA	NA
Histopathological subtypes (Serous vs. Mucinous and othersa)	1.358 (0.896-1.685)	0.712	NA	NA
Depth of invasion (T1-T2 vs. T3-T4)	0.358 (0.235-0.596)	0.015*	0.415 (0.268-0.732)	0.026*
Distant metastasis (Negative vs. Positive)	0.698 (0.425-0.998)	0.625	NA	NA
Histological grade (Low/moderate vs. High)	0.895 (0.562-1.256)	0.846	NA	NA
miR-5195-3p expression (High vs. Low)	0.235 (0.123-0.523)	0.008*	0.368 (0.182-0.632)	0.031*

**P*<0.05; Abbreviations: HR, hazard ratio; CI, confidence interval; OC, ovarian cancer; FIGO Federation International of Gynecology and Obstetrics. aothers: others include the endometrioid, clear cell, and undifferentiated ovarian cancers.

Table 3. Correlations between RHBDD1 expression and clinicopathological characteristics in OC patients.

Patient characteristics	Cases (n=83)	Expression of RHBDD1		*P* value
		High (n=42)	Low (n=41)	
Age				0.228
<55	35	15	20	
≥55	48	27	21	
Tumor size (cm)				0.323
<5	51	28	23	
≥5	32	14	18	
FIGO stage				0.006*
Early (I-IIA)	37	25	12	
Advanced (IIB-IV)	46	17	29	
Tumor differentiation				0.590
Good/moderate	53	28	25	
Poor/undifferentiated	30	14	16	
Histopathological subtypes				0.799
Serous	70	35	35	
Mucinous and othersa	13	7	6	
Depth of invasion				0.225
T1-T2	43	19	24	
T3-T4	40	23	17	
Distant metastasis				0.036*
Negative	45	18	27	
Positive	38	24	14	
Histological grade				0.299
Low/moderate	59	32	27	
High	24	10	14	

**P*<0.05 (p values are calculated with chi-square test); OC, ovarian cancer; FIGO Federation International of Gynecology and Obstetrics. aothers: others include the endometrioid, clear cell, and undifferentiated ovarian cancers.

efficiency in SKOV-3 (Fig. 2A) and OVCAR3 (Fig. 2B) cells. Next, cell proliferation capacity was assessed by CCK-8 assay and colony formation assay. As shown in Figure 2C-D, overexpression of miR-5195-3p inhibited, while knockdown of miR-5195-3p enhanced cell viability in SKOV-3 and OVCAR3 cells. In parallel, SKOV-3 (Fig. 2E) and OVCAR3 (Fig. 2F) cells that overexpressed miR-5195-3p formed fewer colonies than control cells, while those with silenced miR-5195-3p formed more colonies than corresponding control cells. Flow cytometry assays showed that miR-5195-3p overexpression induced cell cycle arrest in G0/G1 phase in SKOV-3 and OVCAR3 cells, while the opposite effects on cell cycle progression were observed in miR-5195-3p-deficient SKOV-3 and OVCAR3 cells (Fig. 2G,H). In addition, Transwell assays demonstrated that the migrating ability of miR-5195-3p mimics groups was suppressed in SKOV-3 and OVCAR3 cells. In contrast, miR-5195-3p downregulation in SKOV-3 and OVCAR3 cells significantly enhanced the number of migratory cells compared with control groups (Fig. 2I). Similarly, miR-5195-3p overexpression inhibited, while knockdown promoted the invasive capacity of SKOV-3 and OVCAR3 cells (Fig. 2J). Overall, these results indicated that miR-5195-3p inhibited OC cell proliferation, migration and invasion *in vitro*.

MiR-5195-3p directly targets RHBDD1

Next, we used the miRNA target prediction algorithm TargetScan to computationally screen genes with miR-5195-3p complementary sites in their 3′-UTR. The results showed that RHBDD1 was a putative target of miR-5195-3p. The miR-5195-3p binding sequences in the 3′-UTR of RHBDD1 mRNA (WT-3′-UTR) or its mutant (MUT-3′-UTR) were subcloned downstream of the luciferase reporter vector (Fig. 3A). As demonstrated by the luciferase reporter assay, the relative luciferase activity of the reporter containing the WT RHBDD1 3′-UTR was significantly decreased when miR-5195-3p mimics were co-transfected, whereas the luciferase activity of the RHBDD1-3′UTR-MUT reporter was unaffected in SKOV-3 (Fig. 3B) and OVCAR3 (Fig. 3C) cells. Moreover, the results from reverse transcription-quantitative PCR (Fig. 3D) and western blot analysis (Fig. 3E) consistently demonstrated that the mRNA and

protein levels of RHBDD1 were significantly downregulated after miR-5195-3p overexpression, while being remarkedly upregulated following miR-5195-3p knockdown in both SKOV-3 and OVCAR3 cells. In addition, we found that RHBDD1 expression level was significantly upregulated in OC tissues as compared to adjacent tissues (Fig. 4A). There was a negative relationship between RHBDD1 expression and miR-5195-3p expression levels in OC tissues (Fig. 4B). As depicted in Table 3, the expression of RHBDD1 was associated with FIGO stage (P=0.006) and distant metastasis (P=0.036).

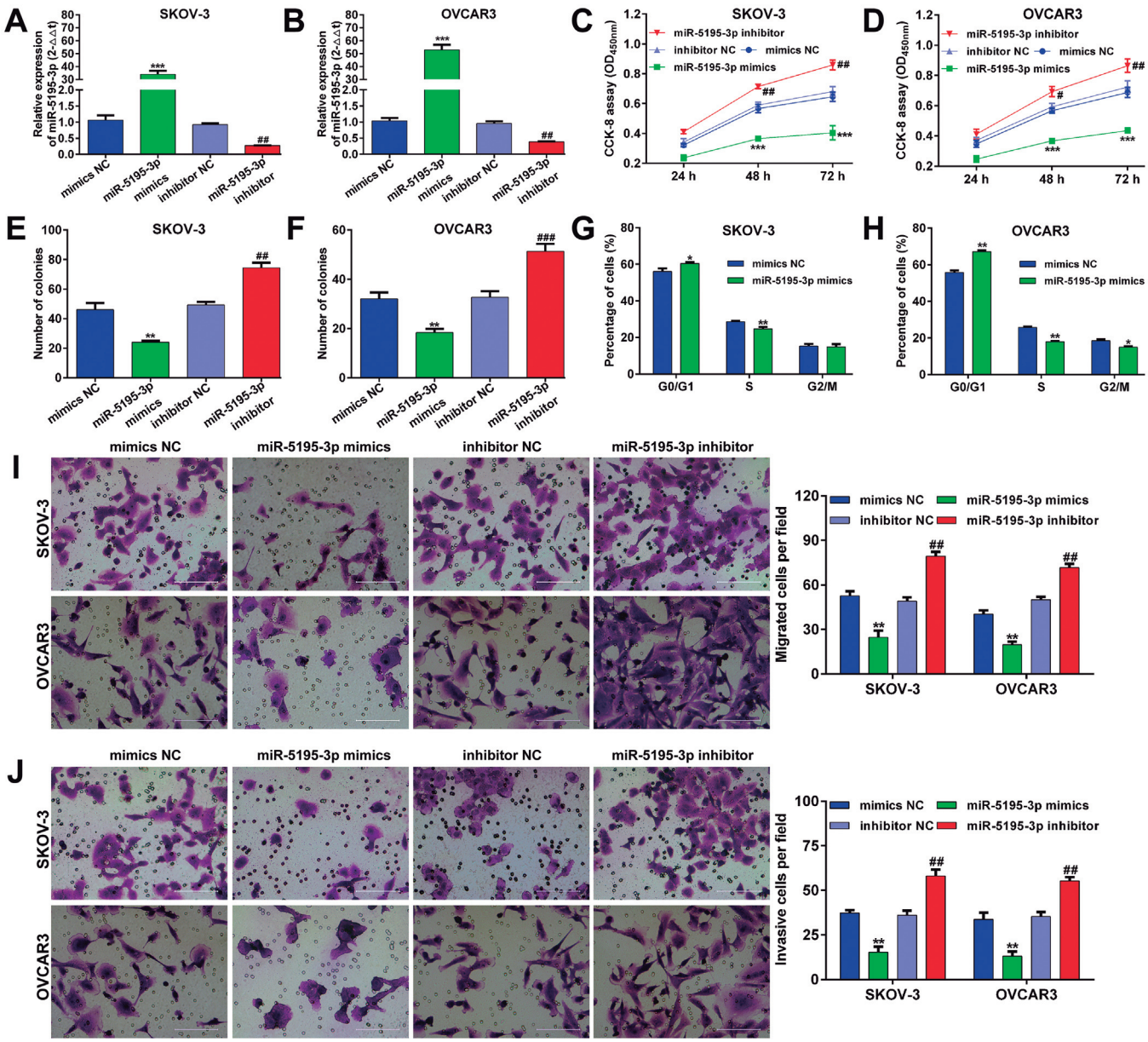

Fig. 2. MiR-5195-3p inhibits the proliferation, migration and invasion in OC cells. SKOV-3 and OVCAR3 cells were transfected with miR-5195-3p mimics and inhibitor, respectively. **A, B.** Relative expression levels of miR-5195-3p in transfected SKOV-3 and OVCAR3 cells. **C, D.** Cell viability was measured at the indicated time points using the CCK-8 assay. **E, F.** Colony formation was measured 14 d after transfection. **G, H.** The transfected SKOV-3 and OVCAR3 cells were stained with PI. Cell cycle distribution was assessed using flow cytometry. Transwell assay was used to analyze cell migration **(I)** and invasion **(J)** capacities in the above transfected OC cells. Comparisons between groups were analyzed using t-tests (two-sided). Differences with P values of less than 0.05 are considered significant. *P<0.05, **P<0.01, ***P<0.001 vs. the mimics NC group; $^{\#}P$<0.05, $^{\#\#}P$<0.01, $^{\#\#\#}P$<0.001 vs. the inhibitor NC group; n=3; Scale bar: 100 μm.

Rescued expression of RHBDD1 abolished the suppressive effects of miR-5195-3p on the phenotypes of OC cells

Considering RHBDD1 as the target of miR-5195-3p in OC cells, we next further investigate whether RHBDD1 upregulation could have effects on OC cell proliferation, migration and invasion. SKOV-3 cells were co-transfected with mimics NC and pcDNA3.1 or pcDNA3.1-RHBDD1, as well as miR-5195-3p mimics and pcDNA3.1 or pcDNA3.1-RHBDD1. The transfection efficiency was confirmed by reverse transcription-quantitative PCR (Fig. 5A) and western blot analysis (Fig. 5B). The results from CCK-8 assay (Fig. 5C) and colony formation assay (Fig. 5D) demonstrated that RHBDD1 overexpression not only promoted cell proliferation, but also reversed the suppressive effects of miR-5195-3p on cell proliferation in SKOV-3 cells. Flow cytometry further confirmed miR-5195-3p induced cell cycle G0/G1 arrest was abolished following RHBDD1 overexpression in SKOV-3 cells (Fig. 5E). Furthermore, RHBDD1 upregulation significantly reversed the miR-5195-3p-imparied migratory and invasive abilities in SKOV-3 cells (Fig. 5F).

MiR-5195-3p served as a tumor suppressor in OC in vivo

To elucidate the functional implication of miR-5195-3p *in vivo*, we established an OC xenograft mouse model by subcutaneously injecting SKOV-3 and OVCAR3 cells transfected with miR-5195-3p mimics or mimics NC into the right flank of nude mice. The representative tumor images in different groups are shown in Figure 6A. The mean volume (Fig. 6B,C) and weight (Fig. 6D) of OC tumors derived from SKOV-3 cells or OVCAR3 cells overexpressing miR-5195-3p were lower relative to mimics NC group. Subsequently, reverse transcription-quantitative PCR was employed to examine the

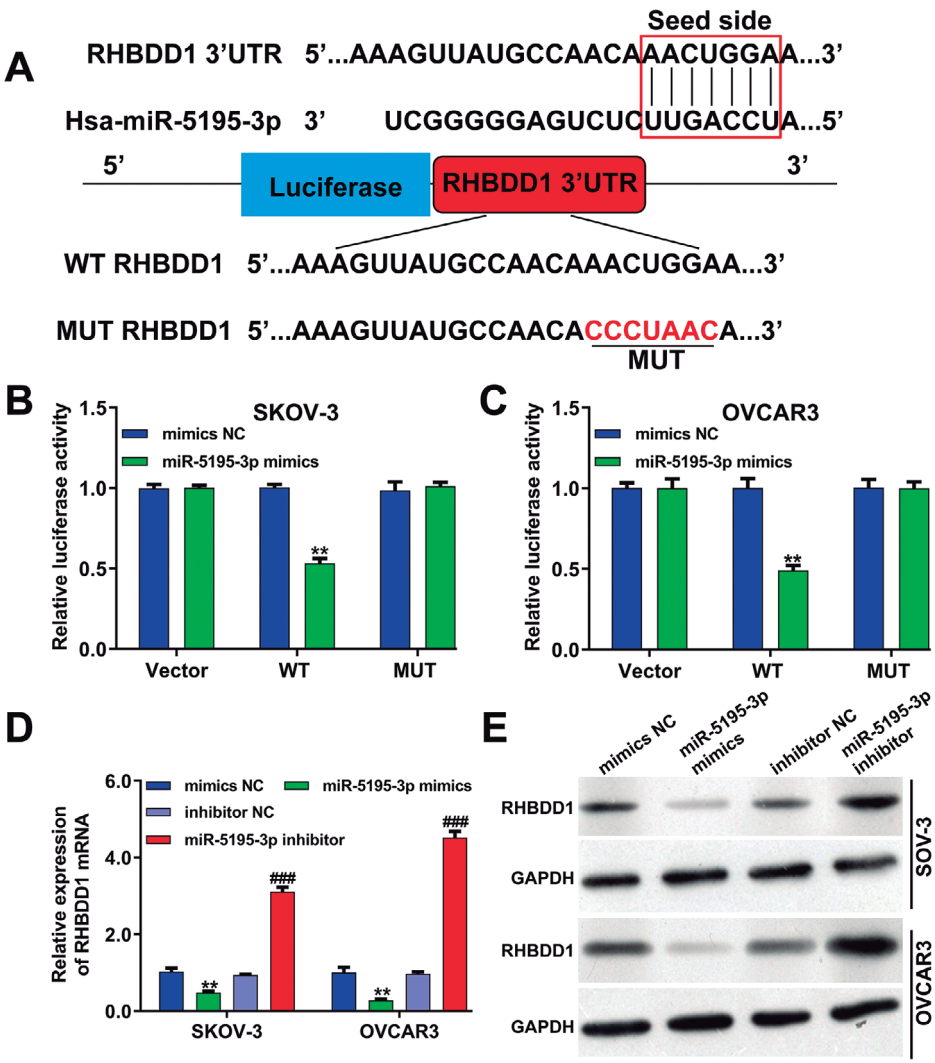

Fig. 3. MiR-5195-3p regulates RHBDD1 expression by binding to its 3′-UTR. **A.** Schematic representation of the RHBDD1 3′-UTR as a direct target for miR-5195-3p. WT or MUT miR-5195-3p targets the RHBDD1 3′-UTR. **B, C.** Luciferase activity was analyzed in SKOV-3 and OVCAR3 cells co-transfected with the WT or MUT RHBDD1 3′-UTR reporter genes and miR-5195-3p mimics or mimics NC. **D.** The mRNA expression of RHBDD1 was analyzed using reverse transcription-quantitative polymerase chain reaction in SKOV-3 and OVCAR3 cells transfected with miR-5195-3p mimics or inhibitor. **E.** RHBDD1 protein expression was analyzed using Western blotting in SKOV-3 and OVCAR3 cells transfected with miR-5195-3p mimics or inhibitor. $^{**}P<0.01$ vs. the mimics NC group; $^{###}P<0.001$ vs. the inhibitor NC group; n=3

expression levels of miR-5195-3p and RHBDD1. The results showed that miR-5195-3p was upregulated (Fig. 6E) and RHBDD1 was downregulated (Fig. 6F) in tumors treated with miR-5195-3p mimics, compared with those treated with the controls. These findings indicated that miR-5195-3p suppressed the growth of OC tumors *in vivo*.

Discussion

Recently, miRNA has become a key player in the development of malignant tumors. Among them, many miRNAs have been found to be abnormally expressed and such abnormal expression often leads to tumorigenesis (Yang et al., 2018). Aberrantly dysregulated miRNAs can be restored by using antagomirs or miRNA mimics (Krutzfeldt et al., 2005; Kota et al., 2009) which established the potential usefulness of miRNAs as therapeutic molecules against cancer. These studies outlined the importance of miRNAs in carcinogenesis. Here, we observed that miR-5195-3p expression was significantly reduced in OC tissues compared with adjacent tissues, which was consistent with previous studies that illustrated that miR-5195-3p was down-regulated in several cancers, including osteosarcoma (Wang et al., 2019), glioma (Yang et al., 2020) and bladder cancer (Jiang et al., 2017). What's more, the survival curves showed that OC patients with low miR-5195-3p p had a poor prognosis, and the Cox regression data demonstrated that miR-

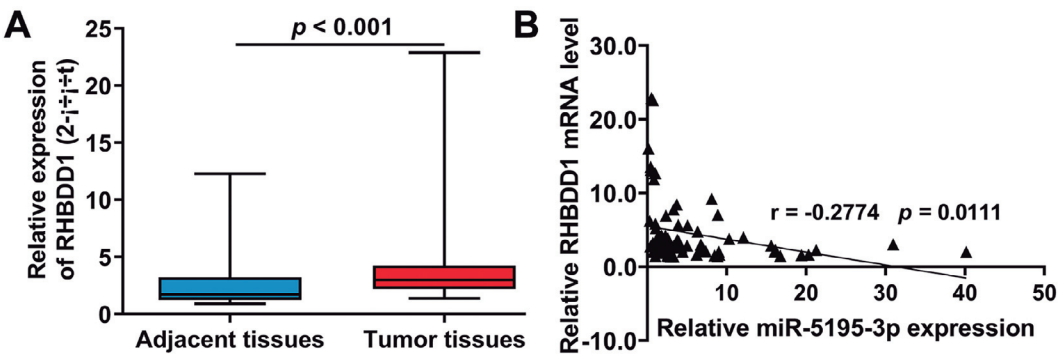

Fig. 4. The relationship between miR-5195-3p and RHBDD1 in OC tissues. **A.** Relative expression of RHBDD1 of ovarian cancer samples and adjacent normal tissues (n=83), assessed by reverse transcription-quantitative polymerase chain reaction. **B.** Pearson's correlation analysis showed the correlation between miR-5195-3p and RHBDD1 in OC tissues.

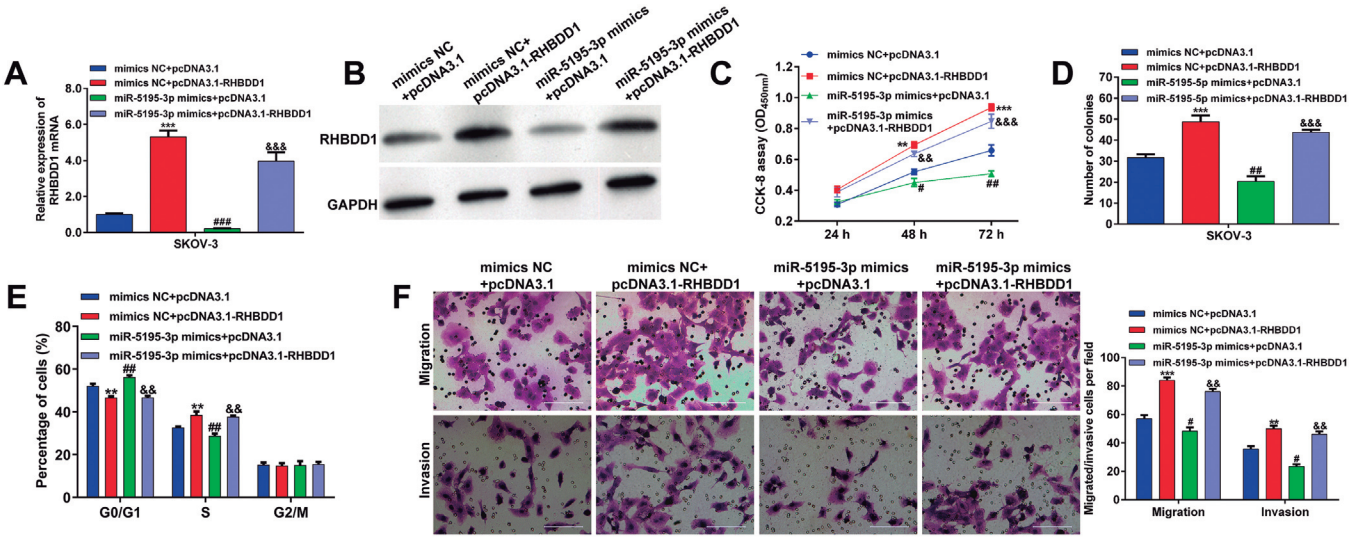

Fig. 5. Rescued expression of RHBDD1 abolished the suppressive effects of miR-5195-3p on the phenotypes of OC cells. SKOV-3 cells were co-transfected with mimics NC and pcDNA3.1 or pcDNA3.1-RHBDD1, as well as miR-5195-3p mimics and pcDNA3.1 or pcDNA3.1-RHBDD1. **A, B.** The expression levels of RHBDD1 in transfected SKOV-3 cells were examined by reverse transcription-quantitative polymerase chain reaction and western blot analysis. **C.** Cell viability was measured at the indicated time points using the CCK-8 assay. **D.** Colony formation was measured 14 d after transfection. **E.** The transfected SKOV-3 cells were stained with PI. Cell cycle distribution was assessed using flow cytometry. **F.** The migratory and invasive properties of the transfected SKOV-3 cells were analyzed using the Transwell assay. Differences with P values of less than 0.05 are considered significant. $^{**}P<0.01$, $^{***}P<0.001$ vs. mimics NC + pcDNA3.1 group; $^{\#}P<0.05$, $^{\#\#}P<0.01$, $^{\#\#\#}P<0.001$ vs. mimics NC + pcDNA3.1 group; $^{\&\&}P<0.01$, $^{\&\&\&}P<0.001$ vs. miR-5195-3p mimics + pcDNA3.1 group; Scale bar: 100μm.

5195-3p might be an independent prognostic indicator for the overall survival of OC patients. Furthermore, we showed that miR-5195-3p inhibited OC cell proliferation, cell cycle progression, migration and invasion *in vitro*, as well as tumor growth *in vivo*. These results indicated the tumor suppressive role of miR-5195-3p in OC, which is in line with its role in NSCLC (Yang, 2019; Li et al., 2021), osteosarcoma (Wang et al., 2019), glioma (Yang et al., 2020) and breast cancer (Liu et al., 2019). Notably, Ebrahimi and Reiisi. (2019) previously found that miR-5195-3p expression level was decreased in OC samples and its reduction was associated with metastasis, which strongly supports our data. Different from it, our study elucidated the functional role of miR-5195-3p in OC *in vitro* and *in vivo*, a more in depth study following the study from Ebrahimi and Reiisi (2019).

To understand the role of miRNA, the identification of its downstream targets is essential. Until now, multiple targets for miR-5195-3p have been identified and validated in previous studies, including GRB10 (Wang et al., 2021), MYO6 (Yang, 2019), EIF4A2 (Liu et al., 2019) and KLF5 (Jiang et al., 2017). Here, we found RHBDD1 was a potential target of miR-5195-3p by bioinformatics analyses. The luciferase activity reporter assay confirmed this prediction. RHBDD1 was previously identified to be upregulated in colorectal cancer (Han et al., 2015; Song et al., 2015; Zhang et al., 2018a) and high RHBDD1 expression as associated with tumor cell growth and metastasis. We found RHBDD1 overexpression promoted OC cell proliferation, migration and invasion in OC cell behaviors. Similarly, decreased RHBDD1 expression reduced cell proliferation and induced cell cycle arrest in human glioblastoma (Wei et al., 2014) and hepatocellular carcinoma (Liu et al., 2013). Knockdown of RHBDD1 inhibited cell proliferation, G1/S phase transition, migration and invasion in breast cancer (Huang et al., 2018; Zhang et al., 2018b). RHBDD1 silencing inhibited cell growth and invasion of NSCLC by mediating ZEB1/PI3K/AKT signaling pathway (Xu et al., 2021). More importantly, we showed that the role of miR-5195-3p on OC cell behaviors was exerted through targeting RHBDD1. In fact, RHBDD1 has been reported to be a direct target of tumor suppressive miRNAs, including miR-138-5p in breast cancer (Zhao et al., 2019), miR-145-5p in colorectal cancer (Niu et al., 2019) and miR-924 in NSCLC (Wang et al., 2020). Here, we identified another miR-5195-3p/RHBDD1 target in OC cells. However, there are some limitations to our study as follows: 1) Rescue experiments in OVCAR3 cells should be performed *in vitro*; 2) The effects of miR-5195-3p inhibitor should be further explored in xenografts *in vivo*; 3) We will validate the oncogenic role of RHBDD1 in an animal model and explore further molecular mechanisms underlying miR-5195-3p/RHBDD1 target.

In summary, our findings indicated that miR-5195-3p suppressed OC cell proliferation, migration, invasion and tumor growth through targeting the expression of

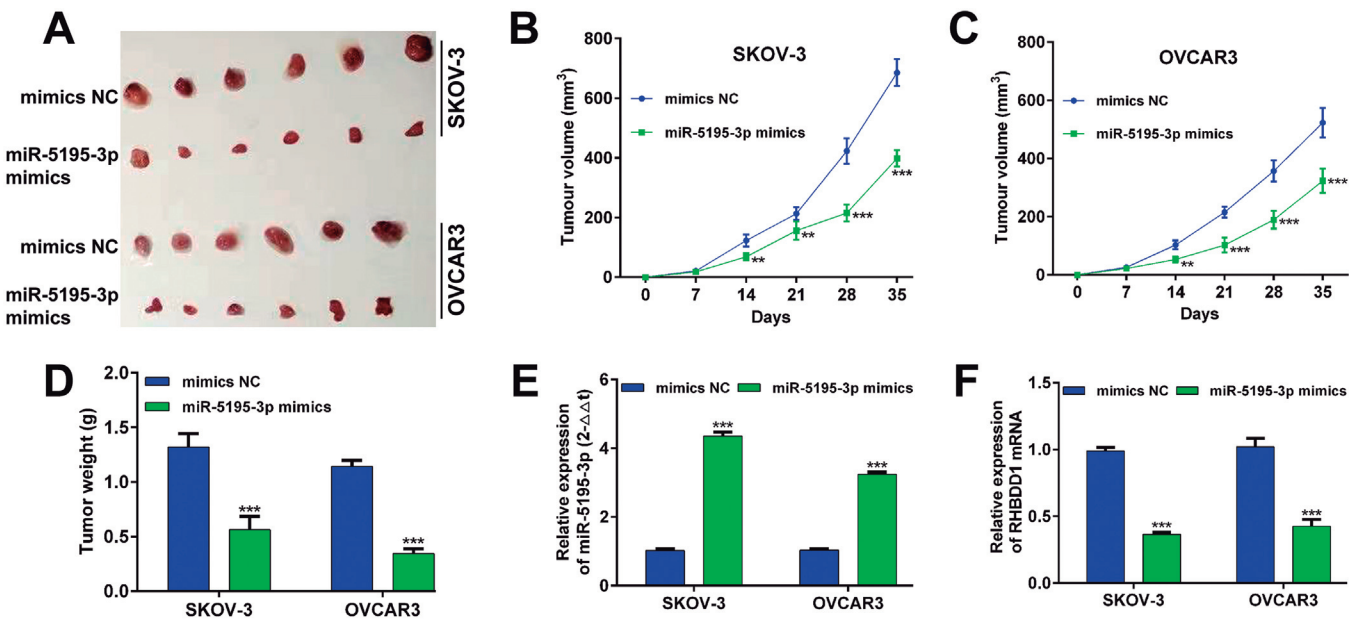

Fig. 6. MiR-5195-3p regressed in-vivo prostate tumor growth. SKOV-3 and OVCAR3 cells were transfected with miR-5195-3p mimics or mimics NC, and then injected subcutaneously into the right flank of nude mice. **A.** Representative tumors from control and experimental mice are presented. **B, C.** Tumor volume was monitored weekly and presented as a mean. Small bar indicates standard error. **D.** Tumor weight was measured and presented as mean. N=6 per group. Relative expression levels of miR-5195-3p **(E)** and RHBDD1 **(F)** were determined in control and experimental tumors analyzed by reverse transcription-quantitative polymerase chain reaction. Differences with *P* values of less than 0.05 are considered significant. ***P*<0.01, ****P*<0.001 vs. mimics NC group

RHBDD1. Our results provide novel insights into the mechanisms underlying the carcinogenesis of OC and may provide novel therapeutic targets for OC treatment.

Ethics approval and consent to participate. This study was approved by the Committee on the Ethics of Fuyang Hospital of Anhui Medical University (Anhui, China). All of the experiments were performed in accordance with the Declaration of Helsinki. All volunteers who donated tissues have provided their written informed consent.

Author contributions. Liang Li and Zhanyu Wang contributed to the conception of the study; Xiaoping Zhang and Yongying Liu contributed significantly to analysis and manuscript preparation; Xiaoyan Shi, Lijun Li and Yun Jia performed the data analyses and wrote the manuscript; all authors helped perform the analysis with constructive discussions; Fangfang Wu and Haosen Cui supervised and checked the manuscript. All authors have read and approved the final manuscript.

Availability of data and materials. All data generated or analyzed during this study are included in this manuscript.

Consent for publication. Not applicable

Funding. Not applicable.

Conflict of interest. The authors declare that they have no conflict of interest.

References

Armstrong D.K., Alvarez R.D., Bakkum-Gamez J.N., Barroilhet L., Behbakht K., Berchuck A., Chen L.M., Cristea M., DeRosa M., Eisenhauer E.L., Gershenson D.M., Gray H.J., Grisham R., Hakam A., Jain A., Karam A., Konecny G.E., Leath C.A., Liu J., Mahdi H., Martin L., Matei D., McHale M., McLean K., Miller D.S., O'Malley D.M., Percac-Lima S., Ratner E., Remmenga S.W., Vargas R., Werner T.L., Zsiros E., Burns J.L. and Engh A.M. (2021). Ovarian cancer, version 2.2020, NCCN clinical practice guidelines in oncology. J. Natl. Compr. Canc. Netw. 19, 191-226.

Boussios S., Mikropoulos C., Samartzis E., Karihtala P., Moschetta M., Sheriff M., Karathanasi A., Sadauskaite A., Rassy E. and Pavlidis N. (2020). Wise management of ovarian cancer: On the cutting edge. J. Pers. Med. 10, 41.

Bracken C.P., Scott H.S. and Goodall G.J. (2016). A network-biology perspective of microRNA function and dysfunction in cancer. Nat. Rev. Genet. 17, 719-732.

Ebrahimi S.O. and Reiisi S. (2019). Downregulation of miR-4443 and miR-5195-3p in ovarian cancer tissue contributes to metastasis and tumorigenesis. Arch. Gynecol. Obstet. 299, 1453-1458.

Freeman M. (2008). Rhomboid proteases and their biological functions. Annu. Rev. Genet. 42, 191-210.

Freeman M. (2014). The rhomboid-like superfamily: Molecular mechanisms and biological roles. Annu. Rev. Cell Dev. Biol. 30, 235-254.

Griffiths-Jones S., Grocock R.J., van Dongen S., Bateman A. and Enright A.J. (2006). MiRBase: MicroRNA sequences, targets and gene nomenclature. Nucleic Acids Res. 34, D140-144.

Han J., Bai J., Yang Y., Yin H., Gao W., Lu A., Liu F., Ge H., Liu Z., Wang J. and Zhong L. (2015). Lentivirus-mediated knockdown of rhomboid domain containing 1 inhibits colorectal cancer cell growth. Mol. Med. Rep. 12, 377-381.

Huang C., Ji X., Peng Y., Wu M., Wu W., Luo Y., Cheng G. and Zhu Y. (2018). Silencing of rhomboid domain containing 1 to inhibit the metastasis of human breast cancer cells *in vitro*. Iran. J. Basic Med. Sci. 21, 1161-1166.

Jiang Z., Zhang Y., Cao R., Li L., Zhong K., Chen Q. and Xiao J. (2017). MiR-5195-3p inhibits proliferation and invasion of human bladder cancer cells by directly targeting oncogene KLF5. Oncol. Res. 25, 1081-1087.

Koole S.N., van Driel W.J. and Sonke G.S. (2019). Hyperthermic intraperitoneal chemotherapy for ovarian cancer: The heat is on. Cancer 125 (Suppl. 24), 4587-4593.

Kota J., Chivukula R.R., O'Donnell K.A., Wentzel E.A., Montgomery C.L., Hwang H.W., Chang T.C., Vivekanandan P., Torbenson M., Clark K.R., Mendell J.R. and Mendell J.T. (2009). Therapeutic microrna delivery suppresses tumorigenesis in a murine liver cancer model. Cell 137, 1005-1017.

Krutzfeldt J., Rajewsky N., Braich R., Rajeev K.G., Tuschl T., Manoharan M. and Stoffel M. (2005). Silencing of microRNAs *in vivo* with 'antagomirs'. Nature 438, 685-689.

Li G., Li X., Yuan C., Zhou C., Li X., Li J. and Guo B. (2021). Long non-coding RNA JPX contributes to tumorigenesis by regulating miR-5195-3p/VEGFA in non-small cell lung cancer. Cancer Manag. Res. 13, 1477-1489.

Liu M., Gong C., Xu R., Chen Y. and Wang X. (2019). MicroRNA-5195-3p enhances the chemosensitivity of triple-negative breast cancer to paclitaxel by downregulating EIF4A2. Cell. Mol. Biol. Lett. 24, 47.

Liu X.N., Tang Z.H., Zhang Y., Pan Q.C., Chen X.H., Yu Y.S. and Zang G.Q. (2013). Lentivirus-mediated silencing of rhomboid domain containing 1 suppresses tumor growth and induces apoptosis in hepatoma HepG2 cells. Asian Pac. J. Cancer Prev. 14, 5-9.

Niu Y., Zhang J., Tong Y., Li J. and Liu B. (2019). MiR-145-5p restrained cell growth, invasion, migration and tumorigenesis via modulating RHBDD1 in colorectal cancer via the EGFR-associated signaling pathway. Int. J. Biochem. Cell Biol. 117, 105641.

Rupaimoole R. and Slack F.J. (2017). MicroRNA therapeutics: Towards a new era for the management of cancer and other diseases. Nat. Rev. Drug Discov. 16, 203-222.

Siegel R.L., Miller K.D. and Jemal A. (2020). Cancer statistics, 2020. CA Cancer J. Clin. 70, 7-30.

Song W., Liu W., Zhao H., Li S., Guan X., Ying J., Zhang Y., Miao F., Zhang M., Ren X., Li X., Wu F., Zhao Y., Tian Y., Wu W., Fu J., Liang J., Wu W., Liu C., Yu J., Zong S., Miao S., Zhang X. and Wang L. (2015). Rhomboid domain containing 1 promotes colorectal cancer growth through activation of the EGFR signalling pathway. Nat. Commun. 6, 8022.

Wang Y., Guan X., Fok K.L., Li S., Zhang X., Miao S., Zong S., Koide S.S., Chan H.C. and Wang L. (2008). A novel member of the Rhomboid family, RHBDD1, regulates BIK-mediated apoptosis. Cell. Mol. Life Sci. 65, 3822-3829.

Wang L., Shi G., Zhu D., Jin Y. and Yang X. (2019). MiR-5195-3p suppresses cell proliferation and induces apoptosis by directly targeting NEDD9 in osteosarcoma. Cancer Biother. Radiopharm. 34, 405-412.

Wang H., Chen X., Yang B., Xia Z. and Chen Q. (2020). MiR-924 as a tumor suppressor inhibits non-small cell lung cancer by inhibiting RHBDD1/Wnt/β-catenin signaling pathway. Cancer Cell Int. 20, 491.

Wang D., Ming X., Xu J. and Xiao Y. (2021). Circ_0009910 shuttled by exosomes regulates proliferation, cell cycle and apoptosis of acute myeloid leukemia cells by regulating miR-5195-3p/GRB10 axis. Hematol. Oncol. 39, 390-400.

Wei X., Lv T., Chen D. and Guan J. (2014). Lentiviral vector mediated

delivery of RHBDD1 shRNA down regulated the proliferation of human glioblastoma cells. Technol. Cancer Res. Treat. 13, 87-93.

Xie H., Wang W., Xia B., Jin W. and Lou G. (2020). Therapeutic applications of PARP inhibitors in ovarian cancer. Biomed. Pharmacother. 127, 110204.

Xu Z., Wang R., Li X., Yang L., Peng H., Wang Y. and Wang P. (2021). RHBDD1 silencing inhibited cell growth and invasion of non-small cell lung cancer by mediating ZEB1/PI3K/AKT signaling pathway. J. Mol. Histol. 52, 503-510.

Yang Q. (2019). MicroRNA-5195-3p plays a suppressive role in cell proliferation, migration and invasion by targeting MYO6 in human non-small cell lung cancer. Biosci. Biotechnol. Biochem. 83, 212-220.

Yang N., Zhu S., Lv X., Qiao Y., Liu Y.J. and Chen J. (2018). MicroRNAs: Pleiotropic regulators in the tumor microenvironment. Front. Immunol. 9, 2491.

Yang J., Yan D.M., Xhu L.X., Si D.M. and Liang Q.H. (2020). MiR-5195-3p inhibits the proliferation of glioma cells by targeting BIRC2. Eur. Rev. Med. Pharmacol. Sci. 24, 267-273.

Yousefi M., Dehghani S., Nosrati R., Ghanei M. and Pasdar A. (2020). Current insights into the metastasis of epithelial ovarian cancer - hopes and hurdles. Cell. Oncol. 43, 1-24.

Zhang M., Miao F., Huang R., Liu W., Zhao Y., Jiao T., Lu Y., Wu F., Wang X., Wang H., Zhao H., Ju H., Miao S., Wang L. and Song W. (2018a). RHBDD1 promotes colorectal cancer metastasis through the wnt signaling pathway and its downstream target ZEB1. J. Exp. Clin. Cancer Res. 37, 22.

Zhang X., Zhao Y., Wang C., Ju H., Liu W., Zhang X., Miao S., Wang L., Sun Q. and Song W. (2018b). Rhomboid domain-containing protein 1 promotes breast cancer progression by regulating the p-Akt and CDK2 levels. Cell Commun. Signal. 16, 65.

Zhao C., Ling X., Li X., Hou X. and Zhao D. (2019). MicroRNA-138-5p inhibits cell migration, invasion and EMT in breast cancer by directly targeting RHBDD1. Breast Cancer 26, 817-825.

Accepted February 20, 2023